

Capacity expansion of solar and wind energy in Europe

Youmi Kim, Robin Krekeler

In order to mitigate climate change, greenhouse gas emission must be substantially reduced. In this report we present a model for the expansion of wind and photovoltaics capacities in Europe at high spatial resolution with the objective to reduce residual load and therefore minimise greenhouse gas emission from the electricity sector. Already installed capacities are considered as well as potentials for maximum expansion under various scenarios. All scenarios resulted in renewable electricity generation covering about 90% of the load. The optimal mix of renewable energy capacities has been quantified as around 75% wind and 25% solar.

Introduction

What is the research challenge addressed by the model? What research questions should it be applied to? What are the possible model outcomes and what is their relevance?

The energy supply sector contributed about 35% to the global anthropogenic greenhouse gas (GHG) emissions in 2010 [1, p. 516]. In order to mitigate climate change, the international community agreed to substantially cut GHG emissions [2]. The transition from fossil-based energy generation towards renewable energy (RE) is and will be a central pillar of mitigating climate change [3].

Since RE source, the relevant policies and geographical restrictions are variable over the regions, pre-planning based on area is essential. In this project we optimised the expansion of renewable energy sources to serve the load of the European power sector based on the Nomenclature of Territorial Units for Statistics level 2 (NUTS-2).

The model presented in the following is based on a study by Zappa and van den Broek [4]. Our model is limited to photovoltaics (PV) and wind energy, its objective is to minimise residual load. 12 different scenarios are simulated depending on possible future developments.

Model

A simplified procedure flow of the project is shown in Figure 1. Data on the potential RE generation and electricity load is pre-processed (see section Data input) to yield the input data for an optimisation problem which we will describe below. The result of this study is an optimised spatial distribution of RE capacities.

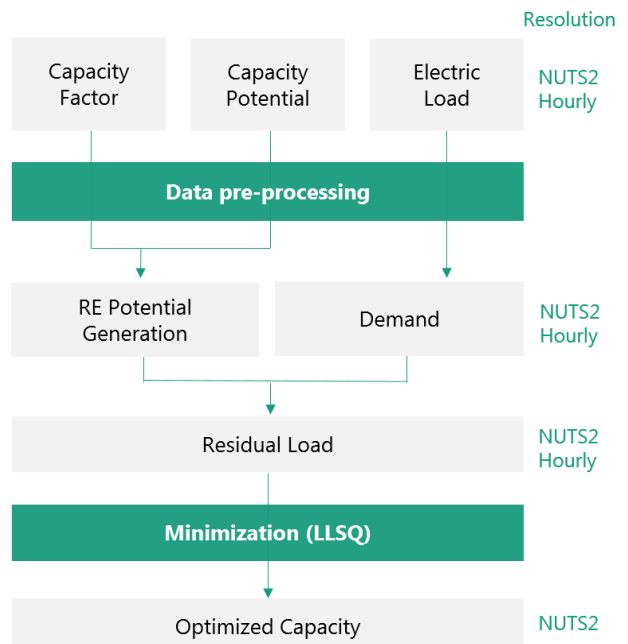


Figure 1 | Process flow of this study.

In the electricity system, balancing power generation and load is crucial in terms of system stability as well as economic considerations. The residual load defined as the difference between generation and demand must be covered by conventional power generation causing GHG emissions. Therefore, the objective function of this study is set by minimisation of the summed square of the residual load z as shown in Equation (2).

The RE generation g_t at timestep t is calculated as the product sum of capacity factors $f_{t,ix}$ and capacity c_{ix} of technology i in region x following Equation (1). The sum over all regions x points to a major assumption of this study: We assume a copper plate Europe and neglect transmission constraints.

$$g_t = \sum_i \sum_x f_{t,ix} \cdot c_{ix} \quad \forall t \quad (1)$$

The installed capacity c_{ix} is our decision variables in the optimisation. The capacity factors $f_{t,ix}$ at timestep t , for technology i in region x are contained in one matrix \mathbf{F} . When multiplied with the vector c containing all capacities c_{ix} one gets the vector of renewable generation \mathbf{g} . The minimisation of the summed square of the residual load \mathbf{r} as the difference between \mathbf{g} and \mathbf{l} is described by Equation (2). The capacity of c_{ix} must be between a minimum capacity c_{ix}^{\min} and a maximum capacity c_{ix}^{\max} . Depending on scenarios, minimum installed capacity c_{ix}^{\min} can be zero or currently (2015) installed RE capacity. Maximum allowed capacity c_{ix}^{\max} equals the potential of each region.

$$\begin{aligned} \min_c & \left(z = \frac{1}{2} \cdot \|\mathbf{Fc} - \mathbf{l}\|_2^2 \right) \\ \text{s.t. } & c_{ix}^{\min} \leq c_{ix} \leq c_{ix}^{\max} \quad \forall i, x \end{aligned} \quad (2)$$

The model described in Equation (2) is a quadratic optimisation but is analytically equivalent to a multiple linear regression with lower and upper bound or linear least square regression (LLSQ). Therefore, it is computable in reasonable time. All pre-processing and calculation of the model are processed in programming language Python.

In reference paper [4], there were more bound constraints are considered such as minimum installed renewable energy capacities for a particular country in order to take into account government policies on variable RE deployment or forced RE penetration rate, which is not considered in this study for simplicity.

Scope

Temporal scope

The simulation is run at hourly resolution for one year. Load \mathbf{l} and capacity factors \mathbf{F} are those of this year. To enhance accuracy and reduce biases from short term weather events longer time durations would be preferred. The temporal scope for this project was set to be one year nonetheless accepting the shortcoming to maintain manageable computation time and data cleaning effort.

Spatial scope

The spatial scope covers 18 countries as depicted in Figure 2. All major EU member states are included. The countries within scope are the intersection of regions covered by the data on the capacity factors and on the capacity potential. More detail on this data is provided in the section Data input.

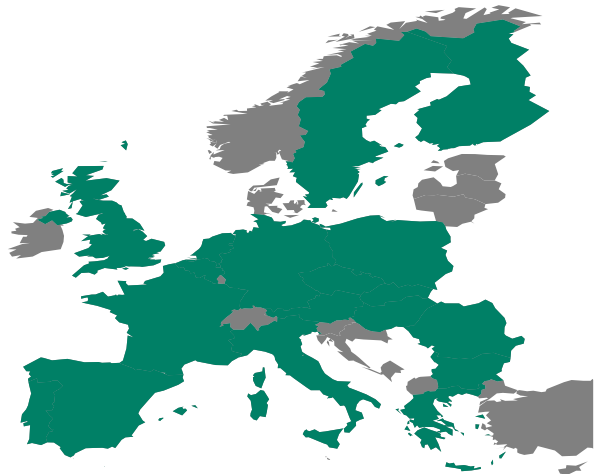


Figure 2 | Countries within scope of this study.

Technologies

The only technologies i within scope are PV and onshore and offshore wind power due to consideration of current technology trends and data availability. Based on installed capacities in 2015 capacity factors $f_{t,ix}$ as an average over all capacities in region x are used. Simulating future expansion of capacities, this approach is biased unless expansion is proportional in spatial and technology distribution to existing capacities for every region respectively. This limitation cannot be expected to hold in reality.

For wind power the aggregation based on actual capacities from 2015 is particularly critical as onshore and offshore wind turbines in one region are aggregated to one average, though it is unrealistic to assume that the fraction of onshore and offshore wind capacities will remain constant with further expansion.

Scenarios

For this project we developed 12 different scenarios differing in minimum capacity c_{ix}^{\min} , the load \mathbf{l}_t , and the potential for expansion of RE capacities c_{ix}^{\max} . Table 1 provides an overview on the scenario definition.

The minimum capacity of technology i in each cell x is either the existing capacity from 2015 or zero for greenfield scenarios.

Table 1 | Scenario definition.

Scenario	Installed RE	Load [TWh/a]	Potential: power density [MW/km ²]	Natural area for PV [%]	Wind power density [MW/km ²]	Wind policy restrictions	max. water depth [m]
1	2015	2859	high	200	5	7	low
2	2015	2859	ref	170	3	5	ref
3	2015	2859	low	140	1.5	3	high
4	2015	4003	high	200	5	7	low
5	2015	4003	ref	170	3	5	ref
6	2015	4003	low	140	1.5	3	high
7	Greenfield	2859	high	200	5	7	low
8	Greenfield	2859	ref	170	3	5	ref
9	Greenfield	2859	low	140	1.5	3	high
10	Greenfield	4003	high	200	5	7	low
11	Greenfield	4003	ref	170	3	5	ref
12	Greenfield	4003	low	140	1.5	3	high

For the load either the actual timeseries from 2015 (2859 TWh in total) or the same timeseries scaled by a factor of 1.4 is assumed. This is to represent expected increase of electricity demand in the future. The 40% increase was assumed based on the highest demand scenario in the reference paper [4, p. 1200]. With increasing electricity demand from new devices like electric vehicles or heat pumps load profiles are expected to change. For the sake of simplicity uniform scaling was applied here, nevertheless.

Regarding the potential for RE expansion 3 scenario branches are considered: reference, low and high potential. These potentials result from power densities assumed for solar and wind respectively, the maximum share of available natural area to be covered with PV capacities, policy restrictions regarding distance to wind farms and maximum water depth for placing offshore wind capacities. For the reference potential default values of the ENSPRESO datasets [5, 6] are used. For the low and high potential all parameters are altered to result in less or more beneficial potentials respectively. Wind policy restriction scenarios in the ENSPRESO data set assume current distance criteria for the reference scenario, most restrictive current policy within the EU for all countries in the high restriction scenario, and least restrictive policy currently observed in the EU for all countries in the low restriction scenario [7, p. 9].

Data input

Most data for this project is taken from two projects of the Joint Research Centre (JRC). This data is available at NUTS-2 level which therefore is the spatial resolution for this study. Freely available sources were chosen for all data required.

Original data

Electricity load

The electricity load at hourly resolution for 2015 in the countries within scope is taken from Open Power Systems Data [8]. These timeseries are based on data from the ENTSO-E transparency platform and pre-processed to be consistent with the ENTSO-E power statistics.

Capacity factors

The JRC provides hourly capacity factors from 1986 until 2015 for PV and wind at NUTS-2 level [9, 10]. This dataset was created under the EMHIRES project. Only the last year of 2015 is used for this analysis. The methodology of the EMHIRES project was designed such that the existing capacity at the end of 2015 is the reference for the capacity factors. This means that the data relates to an average of weather conditions in each NUTS-2 region weighted by the existing capacity of each technology.

The solar capacity factors are simulated based on satellite-recorded radiation data (SARAH). The assumed technology is an open rack south-oriented panel at an inclination of 30°. The simulation results have been verified against actual generation data [9].

For the wind capacity factors reanalysis weather data from the NASA (MERRA). Instead of assumed technology parameters as for PV capacity factors, for wind generation actual wind farm data was used. The capacity factors are calculated based on power curves of the individual turbine types [10].

Capacity potential

The JRC recently published the ENSPRESO dataset [11] of solar, wind [7], and biomass potential in EU-28 countries at NUTS-2 level. Applying geographic information systems land-restriction scenarios were derived and published with little aggregation so policy scenarios, technical restrictions, and power densities can be altered.

Solar capacity is provided as available areas distinguished into different types of roof and façade areas and natural area. In this form the data allows the assumption of different power densities and fraction of natural areas to be utilised [5].

The dataset on wind capacity potential provides power potentials distinguished for quantiles of capacity factors and zones of water depth for offshore turbines based on a power density of 5 MW/km². 3 Scenarios of policy on distance criteria are included [6]. Since capacity factors are given aggregated over each region without distribution the potential provided in quantiles is aggregated for this study. Power density, policy and maximum water depth remain adjustable for scenario definition in the course of our study.

Installed capacities

The installed capacities of PV and wind power generation in each NUTS-2 region are taken from the EM-HIRES project again [9, pp. 33-39, 10, pp. 60-67]. They represent the state at the end of 2015. For PV the capacities published by ENTSO-E at lower spatial distribution were assigned to NUTS-2 regions based on size and solar potential of the region [9, p. 8]. Installed wind capacity at NUTS-2 level is calculated based on locations from actual wind farm data [10, p. 17].

Other data

As proxy for gap filling purposes the area of NUTS-2 regions is required. This data is taken from Eurostat for the year of 2015 [12]. To create offshore wind capacity factors, a list of coastal NUTS regions from Eurostat was used [13].

Data pre-processing

Data gap filling

The load data missed few values which were filled by interpolation for each country for short periods and with values of the previous week for longer durations. The country-specific load data was then aggregated to one central load vector \mathbf{l} .

Data on the capacity potential missed few regions within scope which were taken from similar regions and adjusted for differences in area.

In case of missing data on installed capacities, zero was assumed. This assumption was justified after manually checking the regions of concern which were found to be mostly wind capacities in metropolitan regions.

Creating missing capacity factors

The solar capacity factor data lacked two regions. We decided to fill this data with capacity factors of neighbouring regions. To maintain volatility in the profile and avoid linear dependent columns in \mathbf{F} the time series were filled alternatingly with neighbouring regions for the period of one day. In other words, for the first day the capacity factor was identical to neighbour 1, second day to neighbour 2, and so on, before starting with neighbour 1 again.

In order to create offshore wind capacity factors, the same method was applied with a period length of one week. Coastal regions were referenced as neighbouring regions to the offshore region of each country. This method cannot be expected to be very accurate, as the capacity factors are an average over onshore and offshore turbines, but we believe it is reasonable method for the data available.

Results

In the following we present the results of the reference scenario 2 in detail. It assumes an expansion of installed capacities from 2015, the same load as in 2015 and a reference potential for renewable energies (cf. Table 1). After this an overview of the results of all 12 scenarios is given. The optimised capacity for each NUTS-2 level is calculated and plotted in one map per technology. Solar capacity and wind onshore capacity are plotted in the resolution of NUTS level 2. Wind offshore capacity is plotted in the belonging country. All values are leveled by area as capacity density as well for comparison.

Reference scenario

The reference scenario yields a RE penetration rate α of nearly 90% which is calculated as Equation (3), where r_t is the total RE generation at time t and l_t is total load at time t . The RE capacity consists predominantly of onshore wind (70%), followed by solar capacity (26%) and just a small share of offshore wind capacity. The spatial distribution for these capacities is presented in the following.

$$\alpha = \frac{\sum_t r_t}{\sum_t l_t} \quad (3)$$

Capacity distribution

Onshore wind is comparably evenly distributed over the regions within scope. Figure 3 shows the capacity in each region as a result of the optimisation. High capacities are present in various areas with the highest being southern Portugal, in the highlands of Scotland and south-east Romania.

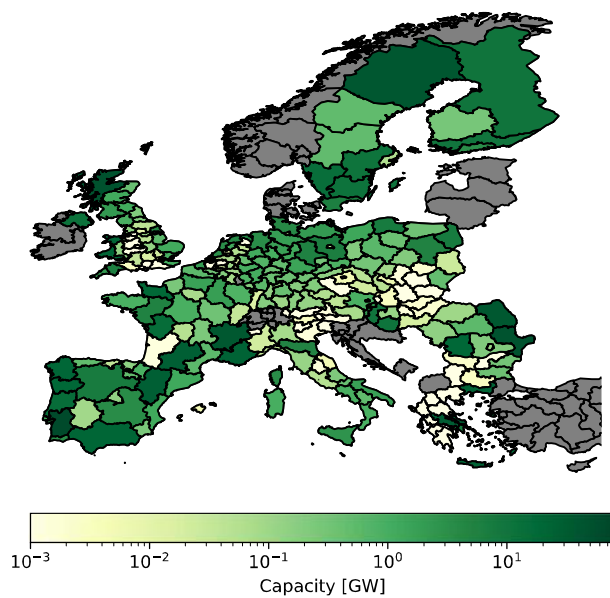


Figure 3 | Onshore wind capacity distribution for the reference scenario.

As the land area of the NUTS-2 regions varies substantially it is worth looking at the capacity density which is capacity divided by area. The capacity density distribution for offshore is shown in Figure 4. The overall pattern remains but a tendency of higher onshore wind capacity deployment in coastal regions becomes clearer.

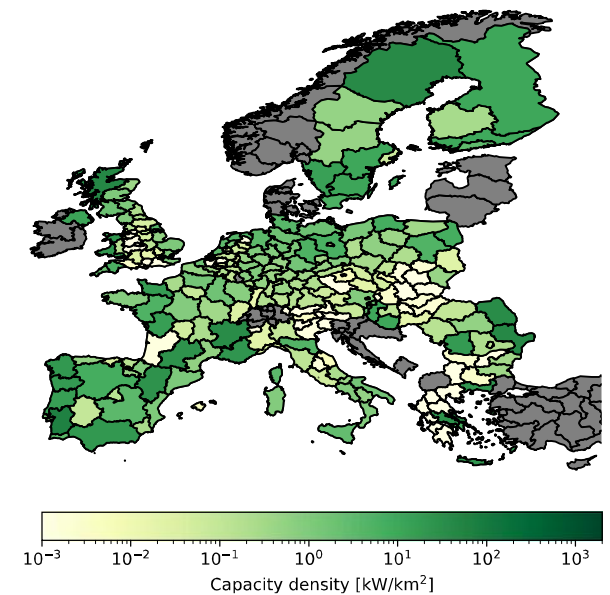


Figure 4 | Onshore wind capacity density distribution for reference scenario.

Regarding offshore capacities significant quantities are deployed in Finland, Poland, Netherlands, Romania and Germany. Figure 5 presents the distribution of offshore capacities among all countries within scope. All Countries not mentioned above have less than 1GW of offshore capacity.

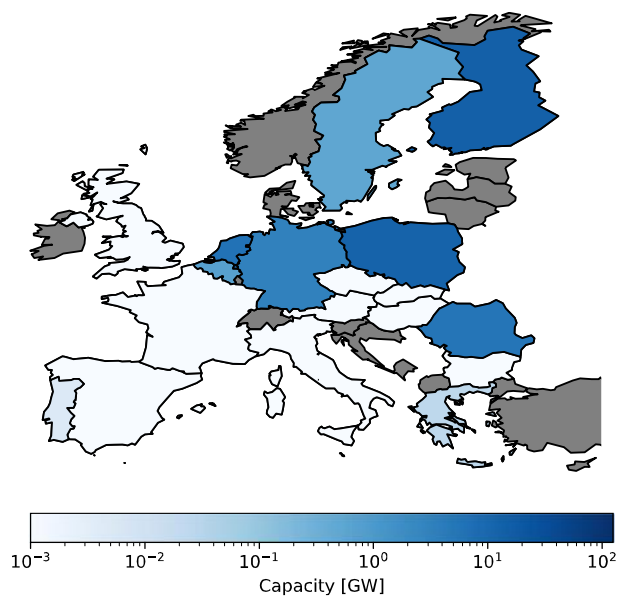


Figure 5 | Offshore wind capacity distribution for the reference scenario.

Solar capacities are deployed in all regions but show some high capacity regions coloured in dark red in Figure 6. Large area regions with low population density in Scandinavia and Scotland have high capacities. In most countries specific regions with high capacities such as Crete in Greece, Limousin in central France or the northeast region of Bulgaria are striking.

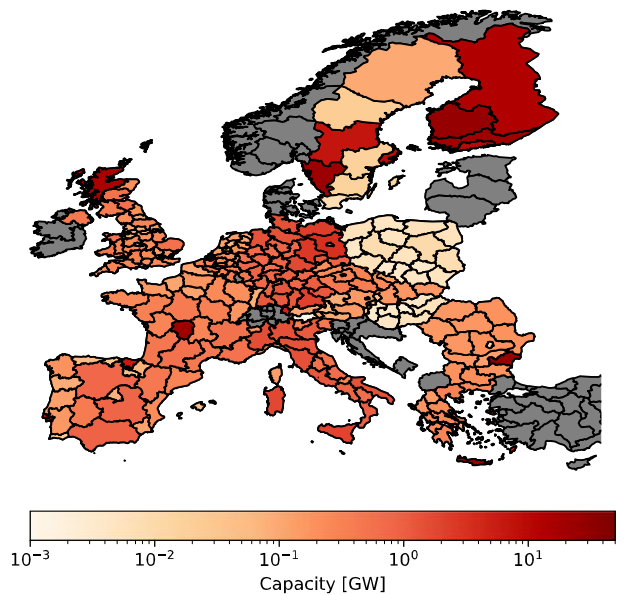


Figure 6 | Solar capacity distribution for reference scenario.

The distribution is more homogeneous when looking at the capacity distribution shown in Figure 6, but the overall pattern remains as described above. Another pattern clearly seen in both capacity and capacity density is the low solar capacity deployment in Poland and Czech Republic.

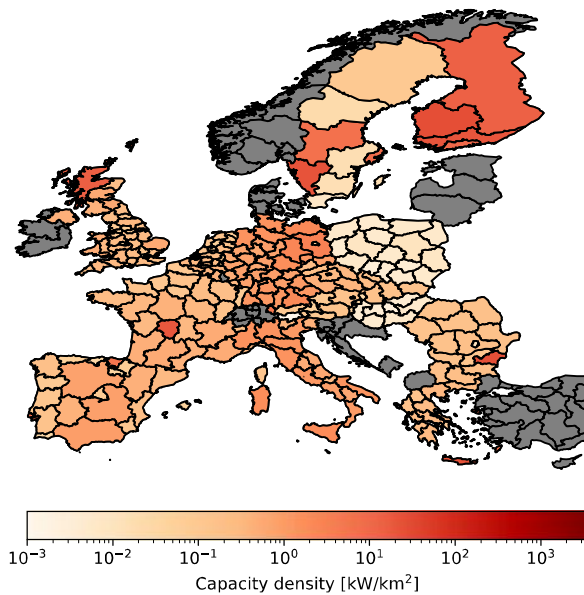


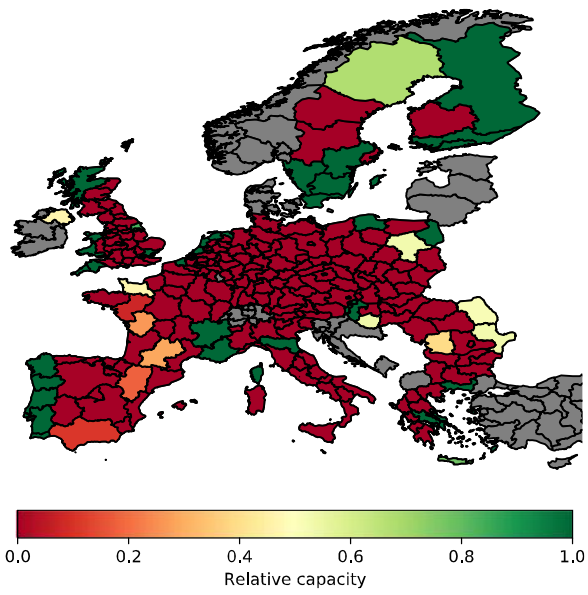
Figure 7 | Solar capacity density distribution for the reference scenario.

Distance to bounds

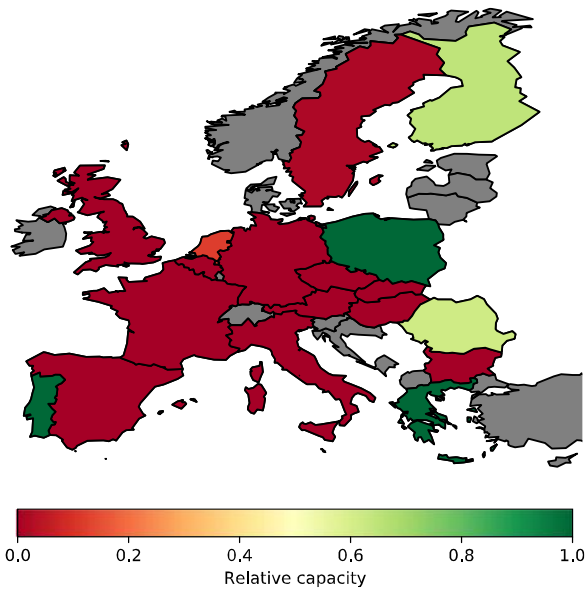
To better understand the reason for the distribution patterns presented before we normalised the expansion of RE capacities to the maximum allowed expansion. This relative capacity \bar{c}_{ix} is calculated according to Equation (4) and can be understood as an indicator for the importance of bounds. Values close to zero (red) indicate regions where capacities are close to the previously installed capacity and values close to one (green) are reached if the capacity is close to the maximum allowed capacity.

$$\bar{c}_{ix} = \frac{c_{ix} - c_{ic}^{\min}}{c_{ix}^{\max} - c_{ic}^{\min}} \quad (4)$$

For onshore wind capacity it can be clearly seen in Figure 8 that in most regions capacities are not expanded significantly above the level of 2015. Nearly all regions with expansion close to the maximum are located at coast. There are very few regions with medium values for the relative capacity where bounds have no impact. Those regions are found primarily in western France and Spain where Onshore wind capacities are expanded without reaching the potential.



As depicted in Figure 9, offshore capacity expansion is only reaching its potential in Greece, Poland and Portugal with Poland being the only country with significant potential under the reference assumptions of this scenario. Finland and Romania reach expansion above 60% of allowed expansion followed by the Netherlands with a relative capacity of 12%.



For the expansion of solar capacity as shown in Figure 10, the potential is constraining for Finland, regions in Sweden, Scotland, Greece, Portugal and Austria. Medium values are seldomly reached as most regions do not expand solar capacities beyond existing quantities.

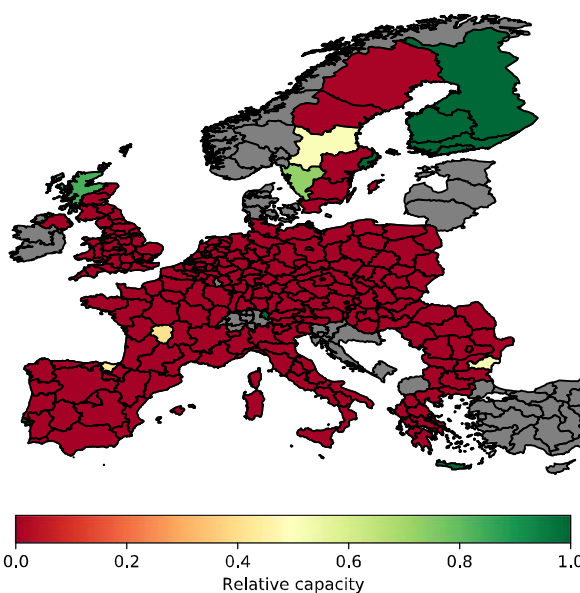


Figure 10 | Relative solar capacity.

Residual load

On average 10% of the load remain uncovered. The residual load is in good approximation normally distributed around an average of 33GW with a standard deviation of 99GW as shown in Figure 11.

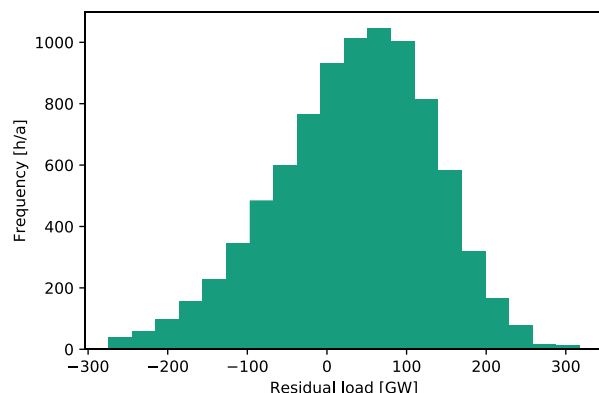


Figure 11 | Histogram of the residual demand in the reference scenario.

The autocorrelation of the residual load shown in Figure 12 clearly shows a seasonal pattern with a daily frequency indicated by the spikes for lags of multiples of 24 hours. In our electricity system model this residual load must be covered by conventional generation.

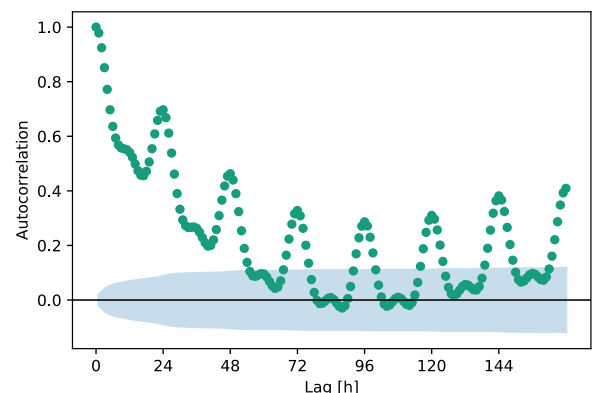


Figure 12 | Autocorrelation of the residual demand in the reference scenario.

This conventional generation can be accompanied by storage also excluded from this study. The average residual load for the hour of the day is shown in Figure 13. Surplus occurs around noon while the highest average residual load is reached in the early evening.

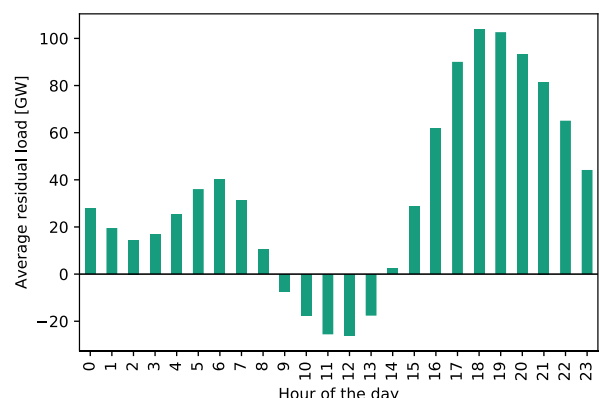


Figure 13 | Average residual load depending on the hour of the day for the reference scenario.

To test how much the remaining load uncovered by RE is a result of constraints it is worth to analyse the relationship between load and residual load shown in Figure 14 as a scatter plot. No significant linear correlation was found ($R^2 = 0.065$). Looking at the graphical representation in Figure 14 other non-linear relationships cannot be identified either.

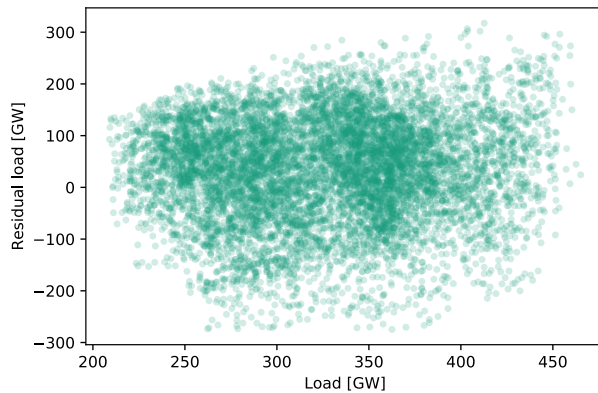


Figure 14 | Relationship between load and residual load in the reference scenario.

All scenarios

The simulation results of all scenarios as summarised in Table 2 (see the annex for maps of the RE capacity distribution for all scenarios). Accumulated capacities for all regions are calculated for each technology. Average and standard deviation of residual load are also calculated. Renewable energy penetration is calculated as Equation (3).

As shown in the maps in the annex, Scandinavian countries like Finland and Sweden and Scottish highland with associated island groups show comparably higher installed capacity for every technology for all scenarios. On the other hand, lowest installed capacity is often spotted in east European countries in general.

Table 2 | Overview of the results of all scenarios.

Scenario	Capacity [GW]			Residual load [GW]		RE penetration [%]
	Onshore wind	Offshore wind	Solar	Mean	Std. deviation	
1	781	135	303	30.2	96.3	90.7
2	882	42	318	33.4	98.8	89.8
3	954	18	341	43.6	104.1	86.6
4	1095	177	429	43.2	135.1	90.6
5	1201	96	448	49.0	139.7	89.3
6	1352	18	525	78.2	149.2	82.9
7	756	136	296	29.6	94.2	90.9
8	853	50	313	32.8	97.0	90.0
9	919	15	339	43.2	103.2	86.8
10	1028	223	426	42.6	133.2	90.7
11	1163	113	441	48.5	138.0	89.4
12	1324	15	520	76.7	148.5	83.2

Capacity for onshore wind stands out in the coastal regions of the study area scope including the Scandinavian countries, Iberian Peninsula and Romania. In case of solar capacity, regions in Finland, Sweden, United Kingdom, France and Romania came out the highest in most of cases.

In general, the ranking of RE technologies with onshore wind having the biggest capacity and offshore wind the least is seen for all scenarios. The RE penetration ranges between 83% (scenario 6) for RE extension with high load and low RE potential and more than 90% for all scenarios with high RE potential.

As shown in Figure 15 the share of solar capacity of the total RE capacity relatively constant around 25% for all scenarios. Major shifts in capacity share take place only between onshore and offshore wind. The higher the RE potential the bigger the share of onshore wind at the expense of offshore wind. This is also true for absolute quantities (cf. Table 2).

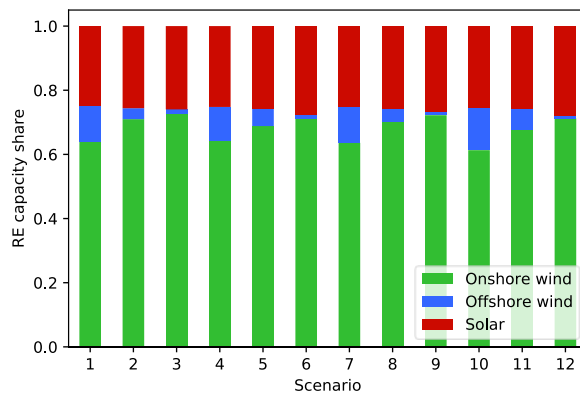


Figure 15 | Share of different RE technologies of total RE capacity for all scenarios.

Figure 16 presents the residual load for all scenarios. The mean is shown as green bars and the standard deviation is depicted as grey lines. When comparing with the scenario definition in Table 1 one sees that the mean residual load increases with increasing load and decreasing RE potential. Variance increases with

increasing RE potential and is unaffected by the load. The standard deviation shown in Figure 16 follows as the product of mean and variance.

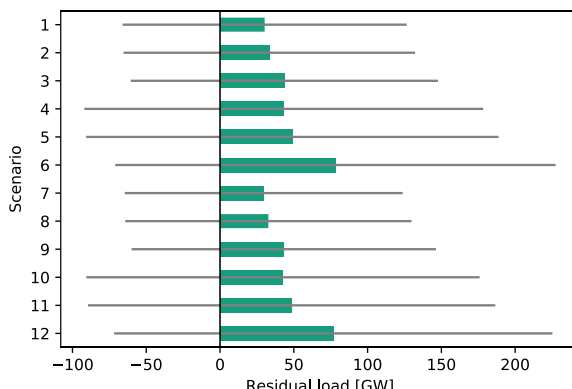


Figure 16 | Residual load for all scenarios (mean: green bars, standard deviation: grey lines).

Discussion

Conclusions from results

One finding consistent throughout all scenarios investigated is the optimal RE penetration α of about 90% when minimising residual load according to Equation (2). Compared to the reference paper [4] ($\alpha = 82\%$) this value is slightly bigger since we applied less constraints. The optimal capacity mix of about 25% solar and 75% wind is equivalent to the findings of Zappa and van den Broek.

The maps of relative capacities revealed that even at very high shares of RE potentials are seldomly exploited. In general distributions of RE capacities were relatively inhomogeneous especially for offshore wind and solar. In most regions capacities are either close to the minimum or maximum capacity. We explain this with the copperplate assumption allowing the solver to choose the best aligning locations without transmission constraints.

Our study also showed that the residual load shows high variance with the standard deviation being in the order of 30% of the average load. This emphasises the need for storage, as the standard deviation of the residual load is about 3 times as big as the average residual load which must be covered by conventional generation. Battery storage might be interesting to balance hourly fluctuations over the course of a day as presented in Figure 13.

Limitations and further enhancements

This model only considers the benefit of temporal generation alignment with the electricity load to minimise residual load. Costs are not reflected by any means. This leads to unrealistic results such as high solar capacity expansion in Finland. The model fits the generation to the load as well as possible and is

blind to poor generation potential. This way those regions with good alignment of capacity factor and load benefit while those regions with worse correlation but better overall generation potential (higher average capacity factor) are disadvantaged.

One way to include cost would be a constraint on the budget which is easily implemented for the cost of leaving behind quick LLSQ algorithms.

The copper plate assumption is a significant simplification of reality. As a precondition for the LLSQ method this assumption is central to this study. Therefore, transmission constraints are hard to include in the existing model architecture.

Another major drawback is the limited number of technologies due to data availability. The model would also work with more technologies such as PV with different orientation or different wind turbine types. Many of the possible enhancements of our model might be connecting points for future projects.

Challenges

Replicating the model of Zappa and van den Broek [4] we were fortunate to find the key data freely available from the JRC. Although this data is fairly well prepared the major effort of this study was tidying and pre-processing the data.

The model quickly reached considerable complexity also due to the high number of scenarios. This led to a very late discovery of a serious modelling error which required much effort towards the end of this project.

References

- [1] IPCC, "Energy Systems," in *Climate Change 2014: Mitigation of Climate Change*, IPCC, Ed., 2014. Accessed: Feb. 9 2020. [Online]. Available: https://www.ipcc.ch/site/assets/uploads/2018/02/ipcc_wg3_ar5_chapter7.pdf
- [2] United Nations, *What is the Paris Agreement?* [Online]. Available: <https://unfccc.int/process-and-meetings/the-paris-agreement/what-is-the-paris-agreement##> (accessed: Feb. 16 2020).
- [3] IPCC, "Introduction," in *IPCC Special Report on Renewable Energy Sources and Climate Change Mitigation*, IPCC, Ed., 2011. Accessed: Feb. 16 2020. [Online]. Available: <https://www.ipcc.ch/site/assets/uploads/2018/03/Chapter-1-Renewable-Energy-and-Climate-Change-1.pdf>
- [4] W. Zappa and M. van den Broek, "Analysing the potential of integrating wind and solar power in Europe using spatial optimisation under various scenarios," *Renewable and Sustainable Energy Reviews*, vol. 94, pp. 1192–1216, 2018, doi: 10.1016/j.rser.2018.05.071.
- [5] European Commission and Joint Research Centre, *EN-SPRESO - solar - pv and csp*. [Online]. Available: <http://data.europa.eu/89h/18eb348b-1420-46b6-978afe0b79e30ad3##> (accessed: Oct. 8 2019).
- [6] European Commission and Joint Research Centre, *EN-SPRESO - wind - onshore and offshore*. [Online]. Available: <http://data.europa.eu/89h/6d0774ec-4fe5-4ca3-8564-626f4927744e##> (accessed: Oct. 8 2019).
- [7] F. Dalla Longa *et al.*, "Wind potentials for EU and neighbouring countries: input datasets for the JRC-EU-TIMES model," JRC technical reports, 2018.

Capacity expansion of solar and wind energy in Europe

- [8] Open Power Systems Data, *Data Package Time series*. [Online]. Available: https://doi.org/10.25832/time_series/2019-06-05## (accessed: Feb. 9 2020).
- [9] I. Gonzalez-Aparicio, T. Huld, F. Careri, F. Monforti, and A. Zucker, "EMHIRES dataset Part II: Solar power generation: European Meteorological derived High resolution RES generation time series for present and future scenarios. Part II: PV generation using the PVGIS model," 2017, doi: 10.2760/044693.
- [10] I. Gonzalez Aparicio, A. Zucker, F. Careri, F. Monforti, T. Huld, and J. Badger, "EMHIRES dataset: Part I: Wind power generation," European Meteorological derived High resolution RES generation time series for present and future scenarios, JRC science for policy report, 2016. Accessed: Oct. 11 2019.
- [11] P. Ruiz *et al.*, "ENSPRESO - an open, EU-28 wide, transparent and coherent database of wind, solar and biomass energy potentials," *Energy Strategy Reviews*, vol. 26, p. 100379, 2019, doi: 10.1016/j.esr.2019.100379.
- [12] Eurostat, *Area by NUTS 3 region*. [Online]. Available: http://appsso.eurostat.ec.europa.eu/nui/show.do?dataset=demo_r_d3area&lang=en## (accessed: Feb. 9 2020).
- [13] Eurostat, *Focus on coastal regions: tables and figures*. [Online]. Available: https://ec.europa.eu/eurostat/statistics-explained/images/6/62/Focus_on_coastal_regions_RYB2012.xls## (accessed: Feb. 15 2020).

Annex

Simulated capacities for all scenarios

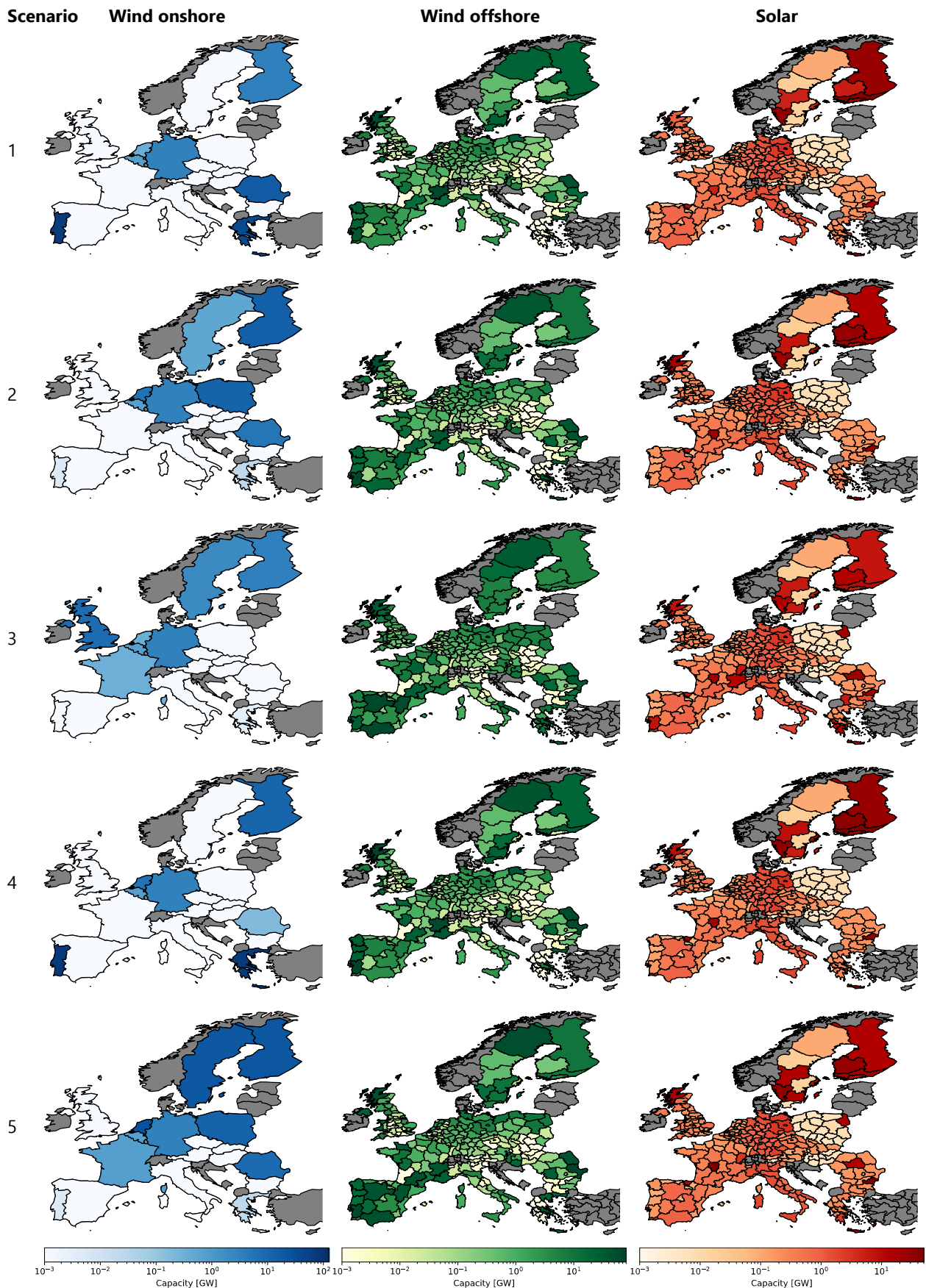


Figure 17 | Spatial distribution of solar and wind capacities for scenarios 1 - 5.

Capacity expansion of solar and wind energy in Europe

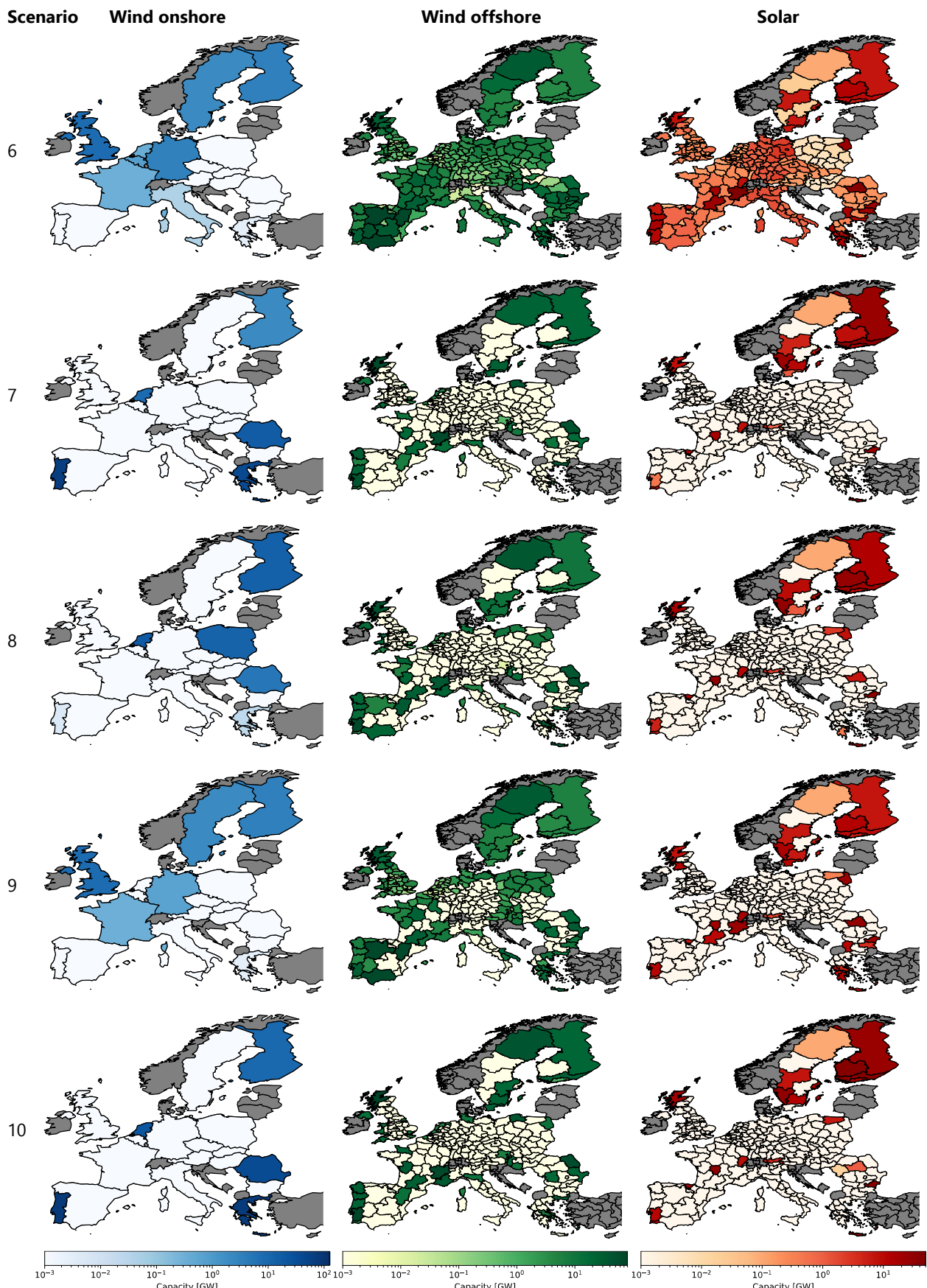


Figure 18 | Spatial distribution of solar and wind capacities for scenarios 6 - 10.

Capacity expansion of solar and wind energy in Europe

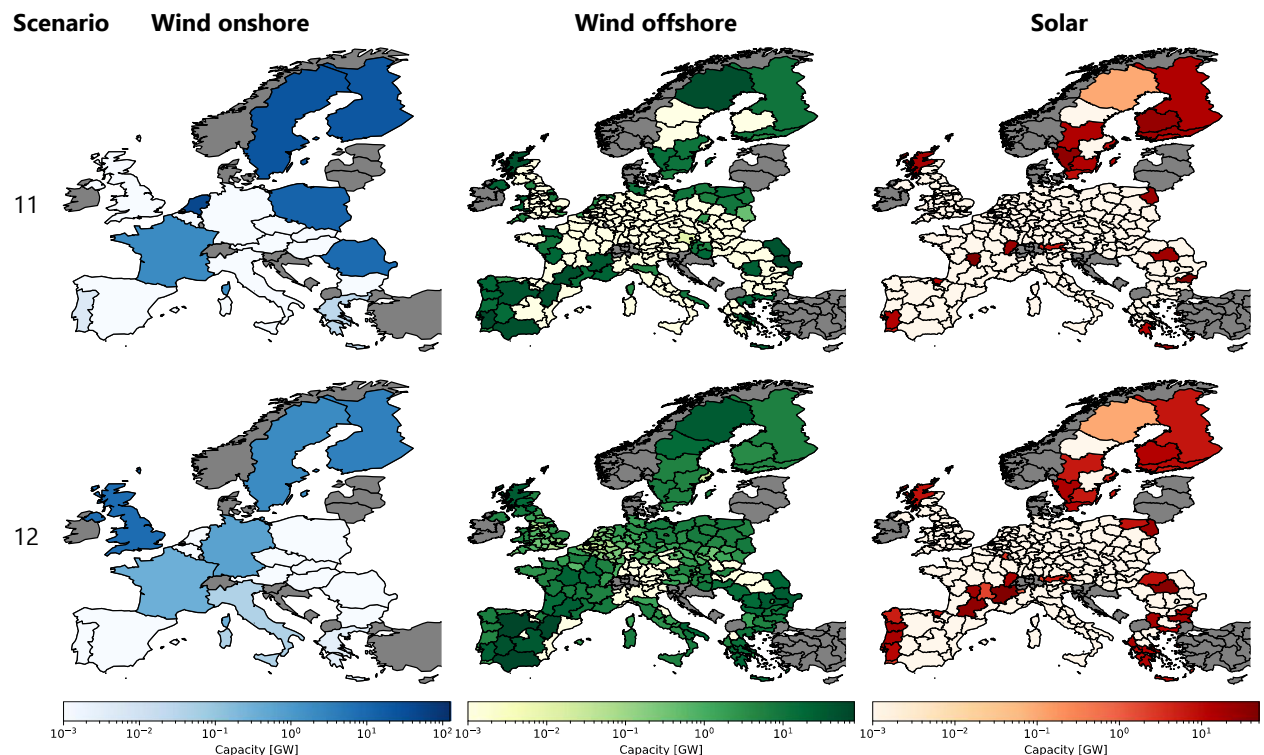


Figure 19 | Spatial distribution of solar and wind capacities for scenarios 11 and 12.